



Combined Strategies for Maintaining Skeletal Muscle Mass and Function in Aging: Myostatin Inactivation and AICAR-Associated Oxidative Metabolism Induction

Marion Pauly, Béatrice Chabi, François Bertrand Favier, Frankie Vanterpool, Stefan Matecki, Gilles Fouret, Béatrice Bonafos, Barbara Vernus, Christine Coudray, Charles C. Coudray, et al.

► To cite this version:

Marion Pauly, Béatrice Chabi, François Bertrand Favier, Frankie Vanterpool, Stefan Matecki, et al.. Combined Strategies for Maintaining Skeletal Muscle Mass and Function in Aging: Myostatin Inactivation and AICAR-Associated Oxidative Metabolism Induction. *Journals of Gerontology Series A: Biological Sciences and Medical Sciences*, 2015, 70 (9), pp.1077 - 1087. 10.1093/gerona/glu147 . hal-01759577

HAL Id: hal-01759577

<https://hal.umontpellier.fr/hal-01759577>

Submitted on 30 May 2022

HAL is a multi-disciplinary open access archive for the deposit and dissemination of scientific research documents, whether they are published or not. The documents may come from teaching and research institutions in France or abroad, or from public or private research centers.

L'archive ouverte pluridisciplinaire **HAL**, est destinée au dépôt et à la diffusion de documents scientifiques de niveau recherche, publiés ou non, émanant des établissements d'enseignement et de recherche français ou étrangers, des laboratoires publics ou privés.

Combined Strategies for Maintaining Skeletal Muscle Mass and Function in Aging: Myostatin Inactivation and AICAR-Associated Oxidative Metabolism Induction

Marion Pauly,^{1,2} Béatrice Chabi,¹ François Bertrand Favier,¹
Frankie Vanterpool,¹ Stefan Matecki,² Gilles Fouret,¹ Béatrice Bonafos,¹
Barbara Vernus,¹ Christine Feillet-Coudray,¹ Charles Coudray,¹
Anne Bonnieu,¹ and Christelle Ramonatxo^{1*}

¹INRA, UMR866 Dynamique Musculaire et Métabolisme, Université Montpellier 1, F-34060, Montpellier, France

²INSERM U1046, Physiology and Experimental Medicine Heart-Muscle Unit, Université Montpellier 1, Université Montpellier 2, Montpellier, France

*Address correspondence to Christelle Ramonatxo, PhD, INRA, UMR866 Dynamique Musculaire et Métabolisme, Université Montpellier 1, F-34060, Montpellier, France. Email: christelle.ramonatxo@univ-montp1.fr

Abstract

Myostatin (mstn) blockade, resulting in muscle hypertrophy, is a promising therapy to counteract age-related muscle loss. However, oxidative and mitochondrial deficit observed in young mice with myostatin inhibition could be detrimental with aging. The aim of this study was (a) to bring original data on metabolic and mitochondrial consequences of mstn inhibition in old mice, and (b) to examine whether 4-weeks of AICAR treatment, a pharmacological compound known to upregulate oxidative metabolism, may be useful to improve exercise capacity and mitochondrial deficit of 20-months mstn KO versus wild-type (WT) mice. Our results show that despite the enlarged muscle mass, the oxidative and mitochondrial deficit associated with reduced endurance running capacity is maintained in old mstn KO mice but not worsened by aging. Importantly, AICAR treatment induced a significant beneficial effect on running limit time only in old mstn KO mice, with a marked increase in PGC-1 α expression and slight beneficial effects on mitochondrial function. We showed that AICAR effects were autophagy-independent. This study underlines the relevance of aged muscle remodelling by complementary approaches that impact both muscle mass and function, and suggest that mstn inhibition and aerobic metabolism activators should be co-developed for delaying age-related deficits in skeletal muscle.

Key Words: PGC-1 α —Endurance—Mitochondrial function—AMPK—Autophagy

The identification of the myostatin (mstn) protein, a member of the transforming growth factors (TGF β) family that is expressed in skeletal muscle, has brought much interest for mstn inhibition as a

treatment of muscle-wasting disorders such as sarcopenia. Indeed, genetic alteration of this negative regulator of muscle growth led to a hypermuscular phenotype in many animal species and in a human

study (1) suggesting that manipulation of mstn can be beneficial for maintaining muscle mass in aged individuals. Previous studies have shown that an acute mstn inhibition using the antibody PF-354 in 24-month-old mice significantly improved muscle weight (2) and that genetic ablation of mstn attenuated age-related skeletal muscle atrophy (3,4). The effect of mstn inhibition on muscle contractile properties is less evident. Early studies reported that specific tension (ratio of force to mass), a marker of the muscle contractile efficiency, is reduced in mstn null mice (KO) compared to their wild-type (WT) littermates (5–7). However, a recent study showed that the hypertrophic muscle, that develops as a consequence of propeptide-mediated inhibition of mstn in aged mice, has normal contractile properties (8). Moreover, other studies have reported that inhibiting mstn expression is instrumental in preventing age-related pathological alterations in heart function (9) or rescuing aged-related osteoporosis and insulin sensitivity in senescent mice (10). Collectively, these observations suggest that mstn blockade may provide an effective therapy to attenuate the skeletal muscle function deficit (11), enhancing muscle mass and whole body metabolism in aged mammals (2).

Loss of mstn expression in young mice is also associated with specific metabolic features in skeletal muscle (12). Early studies provided evidence at the cellular level that loss of myostatin leads, despite the enlarged muscle mass, to loss of oxidative properties, with impaired activity of oxidative enzymes, mitochondrial DNA depletion, and a reduced capillary density (5,13,14). Further evidence about the metabolic deregulation of the mstn-deficient muscle was provided by our data showing uncoupling in the intermyofibrillar mitochondria respiration in young mstn KO glycolytic muscles, associated with increased muscle fatigability during *ex vivo* contractility tests (15). As discussed recently, collectively the above studies on muscle physiology in the absence of myostatin or with myostatin inhibition make the point that the cost for the induced hypermuscularity is an oxidative and mitochondrial metabolic deficit (12,16). While attenuating myostatin signaling is considered as a very attractive strategy to halt and possibly reverse age-related muscle weakness (12), few studies are available on the metabolic muscle status in aged mice with myostatin inhibition. A recent report demonstrates a shift toward a hypermuscular glycolytic phenotype in 20-month-old animals with propeptide-mediated inhibition of myostatin and highlights a decrease in the expression of key genes that control ubiquitin-mediated protein breakdown (8). The impact on oxidative, mitochondrial metabolism, and consequences on endurance muscle capacity remains to be investigated.

The oxidative and mitochondrial deficit with myostatin inhibition that may be worsened with aging raised the interest of activating mitochondrial biogenesis and oxidative metabolism to improve function of aged mstn-deficient muscle and to potentiate the mstn inhibition therapeutic strategy. Interestingly, reports by Patel's group provided key findings that the mstn-deficient muscles are not genetically locked and can be functionally remodeled toward oxidative metabolism by means of exercise training (17,18). In such conditions as age, the use of exercise mimetic drug may represent an interesting alternative therapeutic strategy to boost aerobic metabolism (17). In this context, the synthetic agonist AICAR (5-aminoimidazole-4-carboxamide-1-D-ribofuranoside), up-regulates oxidative metabolism and mimics the effects of aerobic exercise in young skeletal muscle (19). Indeed, this targeting key pharmacological molecule induces the activation of AMP-activated protein kinase (AMPK), a major sensor of cellular energy status and consequently increases the expression and phosphorylation of peroxisome proliferator-activated receptor

gamma coactivator 1 alpha (PGC-1 α) (20). AMPK regulates expression of proteins involved in energy metabolism including glucose and fatty acids transporters, GLUT4 and FAT/CD36 respectively (21,22). PGC-1 α is considered as the master regulator of mitochondrial biogenesis, regulating several co-transcription factors to induce the expression of nuclear genes encoding mitochondrial protein (23,24). Moreover, it has been shown, that AICAR switches on autophagy-mitophagy pathway, a mechanism that ensure mitochondrial quality control through the removal of damaged or dysfunctional mitochondria (25,26).

The novelty of the present work is to test an emerging strategy: to remodel aged muscle with co-simultaneous loss-muscle mass inhibition and aerobic metabolism activation. The aim of this study was thus to bring original data on metabolic and mitochondrial consequences of mstn inhibition in old mice and to determine whether AICAR treatment, may be useful to improve exercise capacity and mitochondrial deficit of aged WT and mstn KO mice.

We show that (a) the oxidative and mitochondrial deficit is maintained but not worsened by aging in old mstn KO mice compared to WT, (b) AICAR treatment had no beneficial impact on skeletal muscle of WT mice and could not be considered as a mimetic of exercise in aged mice, and (c) AICAR treatment improved aerobic running capacity in aged mstn KO mice with a marked increase in PGC-1 α expression and slight beneficial effects on mitochondrial function.

Methods

Animals

Male mstn KO mice used in this study have been described previously (27). Twenty-month old male mstn KO and wild-type (WT) mice ($n = 17$ – 19 /genotype) were randomly divided in two groups comprising vehicle-treated (WT+placebo and KO+placebo) and AICAR-treated (WT+AICAR and KO+AICAR) animals ($n = 8$ – 10 /group). Mice were treated with either vehicle (0.9% NaCl) or AICAR (Toronto Research chemicals, Toronto, ON, Canada) at a daily dose of 500 mg/kg body weight by intra-peritoneal injection (5/7 days per week) during 4 weeks. Mice were fed ad libitum and kept under a 12:12-h light-dark cycle. The experimental protocols of this study were handled in strict accordance with European directives (86/609/CEE) and approved by the Ethical Committee of Region Languedoc Roussillon.

Performance Outcomes

At the beginning and the end of AICAR or placebo treatment, mice were submitted to two treadmill running tests in a blinded manner. Maximal aerobic velocity (MAV) was determined via a running test, where the speed was gradually increased by 2 m/min from 10 m/min until exhaustion. Exhaustion was defined when the mice were no longer able to maintain their normal running position and/or after 5 consecutive seconds in contact with the shock grid (≤ 0.2 mA) at the rear of the treadmill. Endurance capacity was determined via a submaximal running test where the speed starts at 10 m/min for the first 2 minutes and was set to 70% of maximal running speed until exhaustion. The limit endurance time was recorded. Mice were killed 48 hours after the last running test.

Mitochondrial Isolation

One hour after the last AICAR injection, mice were killed by cervical elongation. Gastrocnemius, soleus, extensor digitorum longus (EDL) muscles were removed, weight and quickly frozen in liquid nitrogen

and stored at -80°C for western blotting and enzymatic analysis. Tibialis anterior, gastrocnemius, and quadriceps were immediately placed in ice-cold buffer (100 mM KCl, 5 mM MgSO_4 , 5 mM EDTA, and 50 mM Tris-HCl, pH 7.4). Subsarcolemmal (SS) and intermyofibrillar (IMF) mitochondria were fractionated by differential centrifugation as described previously (28). Mitochondria were resuspended in 100 mM KCl and 10 mM MOPS, pH 7.4. Mitochondrial protein content was determined using the Bradford assay and the yield was expressed as milligram of mitochondrial proteins per gram of muscle wet weight.

Mitochondrial Respiration

SS and IMF mitochondria oxygen consumption was measured using the high-resolution Oxygraph-2k (OROBOROS Instruments, Innsbruck, Austria). Mitochondrial subfractions were incubated in two sealed thermostated chambers (37°C) containing 2 mL of MIRO5 respiration medium [0.5 mM EGTA, 3 mM $\text{MgCl}_2 \cdot 6\text{H}_2\text{O}$, 65 mM KCl, 20 mM taurine, 10 mM KH_2PO_4 , 20 mM HEPES, 110 mM sucrose, and 1 g/l BSA, pH 7.1]. Resting rate (state 4) was evaluated in the presence of 5 mM glutamate, 2.5 mM malate, and 5 mM succinate; ADP-stimulated rate (state 3) was determined after addition of 0.5 mM ADP. Mitochondria integrity was checked using NADH addition during state 3 measurements. The increase in respiration was less than 10% and not significantly different between WT and KO mice, showing that mitochondria were fully functional (data not shown). Data acquisition and analysis was performed using Oxygraph-2k-DatLab software version 4.3 (OROBOROS Instruments). The respiratory control ratio (RCR) was set as the ratio of oxygen consumption at state 3 over oxygen consumption at state 4.

Mitochondrial Enzymes Activities

Mitochondrial activities were measured in gastrocnemius muscle. Citrate synthase (CS) activity was measured as previously described (29): the activity of the enzyme was measured spectrophotometrically at 412 nm by following the yellow color of 5-thio-2-nitrobenzoic acid, which is generated from the reaction of 5,5'-dithiobis-2-nitrobenzoic acid with the free Co-A liberated from the reaction of acetyl-CoA and oxaloacetate under citrate synthase action to synthesize citrate. Complex I (CI) activity was measured as previously described (28): the method is based on measuring spectrophotometrically at 600 nm 2,6-dichloroindophenol reduction by electrons accepted from decylubiquinol, reduced after oxidation of NADH by complex I. Complex II (CII) and complex II+ III (CII+III) activities were measured as previously described: succinate-ubiquinone reductase and succinate-cytochrome *c* reductase activity were, respectively, determined spectrophotometrically at 600 nm and 550 nm (31). Cytochrome *c* oxidase (COX) activity was measured as previously described: oxidation of reduced cytochrome *c* is followed spectrophotometrically at 550 nm (15).

Western Blotting

Frozen EDL muscle samples were homogenized using an Ultra Turrax homogenizer in an ice cold extraction buffer (20 mM HEPES, pH 7.4, 2 mM EGTA, 50 mM β -glycerophosphate, 1 mM dithiothreitol, 1 mM Na_3VO_4 , 10% glycerol, 1% Triton X-100, 10 μM leupeptin, 5 μM pepstatin A, 3 mM benzamidine, 10 $\mu\text{g}/\text{mL}$ aprotinin, and 1 mM phenylmethylsulfonyl fluoride). Proteins (50 μg) were separated on SDS-PAGE and then transferred to a nitrocellulose membrane (120 minutes, 120 V). Membranes were blocked in

TBS1X/0.2% Tween-20 containing either 5% fat-free milk or 5% BSA for 1 hour at room temperature. Then, membranes were incubated overnight with primary antibody against, phospho-AMPK α (Thr172), total AMPK α , phospho-ACC (Ser79), total ACC, LC3, Beclin-1, p62 (1/1000; Cell Signaling Technology, Danvers, MA), PGC-1 α (1/1000; Calbiochem, Merck, Darmstadt, Germany), VDAC (1/2000; Abcam, Cambridge, UK), mitochondrial respiratory complex subunits (I-20 kDa; II-30 kDa; III-47 kDa; V-53 kDa; 1/208; MitoSciences, Eugene), α -tubulin (1/6000; Sigma-Aldrich, St Louis, MO), GAPDH (1/60000; Abcam), FAT/CD36 (1/500; Abcam), GLUT4, GRP78 (1/500; SantaCruz Biotechnology, Santa Cruz, CA) in blocking buffer. After washes in TBS1X/0.2% Tween-20 under gentle agitation, membrane was incubated for 1 hour with horseradish peroxidase-labelled antibody. After further washes, antibody-bound proteins were revealed using enhanced chemiluminescence detection reagents (ECL, ThermoScientific, Courtaboeuf, France). α -tubulin and GAPDH were used as loading references and blot intensities were measured using the ImageJ software (NIH).

Statistical Analysis

All data are presented as means \pm SEM. Unpaired Student's *t*-tests were used to indicate statistical difference between the two aged groups of mice. A two-way ANOVA followed by Bonferroni multiple-comparison procedure was used to determine the effects of AICAR treatment and animal genotype mice. To facilitate the reading of AICAR effect, we presented separated analysis on WT and KO cohorts and reported in figures' legend the results of ANOVA. Data are thus presented as the fold increase in AICAR over placebo group for each genotype. No AICAR effect was thus visualized by the dashed line, arbitrary taken as 1. Above this value, AICAR overexpressed or stimulated, under this value, AICAR underexpressed or depreciated. The significance level was set at 0.05. The data were analyzed using the statistical package Graphpad Prism.

Results

Aged mstn KO Mice Conserved the Hypermuscular Phenotype Coupled With a Glycolytic Phenotype Compared to Aged WT Mice

Body and skeletal muscle (quadriceps, gastrocnemius, tibialis anterior, EDL, soleus) weights were significantly greater in aged mstn KO mice compared to their WT littermates (Table 1), confirming the hypermuscular phenotype maintenance. Muscle hypertrophy reached about 140% for glycolytic muscles and 171% for the oxidative muscle soleus in aged mstn KO mice compared to aged WT. Concerning metabolic markers, aged mstn KO EDL muscle showed a significant increase in GLUT4 protein levels, and a decrease in FAT/CD36 protein levels compared to aged WT mice (Figure 1A).

Aged mstn KO Mice Presented a Reduction in Oxidative Metabolism and in Mitochondrial Pool Associated With an Impairment of Aerobic Running Performance

EDL muscle showed a significant decrease in PGC-1 α protein levels in KO mice compared to WT mice (Figure 1B). We did not detect any differences between the two groups in phosphorylation of AMPK (Figure 1B), nor in phosphorylation of ACC (acetyl CoA carboxylase), its downstream target (data not shown). In addition, aged mstn KO mice exhibited a decrease in protein level of the outer

Table 1. Body and Muscle Weights in Aged WT and *mstn* KO Mice

	Body Weight	TA/BW	EDL/BW	QUAD/BW	GASTRO/BW	SOL/BW	PLANT/BW	Heart/ BW
WT+Placebo	35.0 ± 4.2	1.49 ± 0.24	0.37 ± 0.11	6.19 ± 0.96	4.99 ± 0.97	0.21 ± 0.03	0.96 ± 0.08	5.23 ± 0.63
KO+Placebo	42.2 ± 4.1*	2.34 ± 0.22*	0.53 ± 0.08*	8.71 ± 0.72*	7.16 ± 0.63*	0.36 ± 0.06*	1.40 ± 0.10*	3.87 ± 0.78*
WT+AICAR	35.9 ± 5.3	1.51 ± 0.26	0.32 ± 0.08	5.48 ± 0.73	4.41 ± 0.58	0.024 ± 0.06	0.97 ± 0.36	4.70 ± 0.39
KO+AICAR	41.6 ± 5.5*	2.54 ± 0.17*	0.51 ± 0.07*	8.51 ± 1.11*	6.71 ± 0.70*	0.37 ± 0.10*	1.47 ± 0.22*	4.25 ± 0.78*

Data are expressed as means ± SEM. BW: Body weight (g); Gastro: gastrocnemius; Quad: quadriceps; TA: tibialis anterior; EDL: extensor digital longus; SOL: soleus. Muscle weights are normalized by BW (mg/g). * $p < .05$ KO versus WT (ANOVA genotype main effect); $n = 8-10$ in each group.

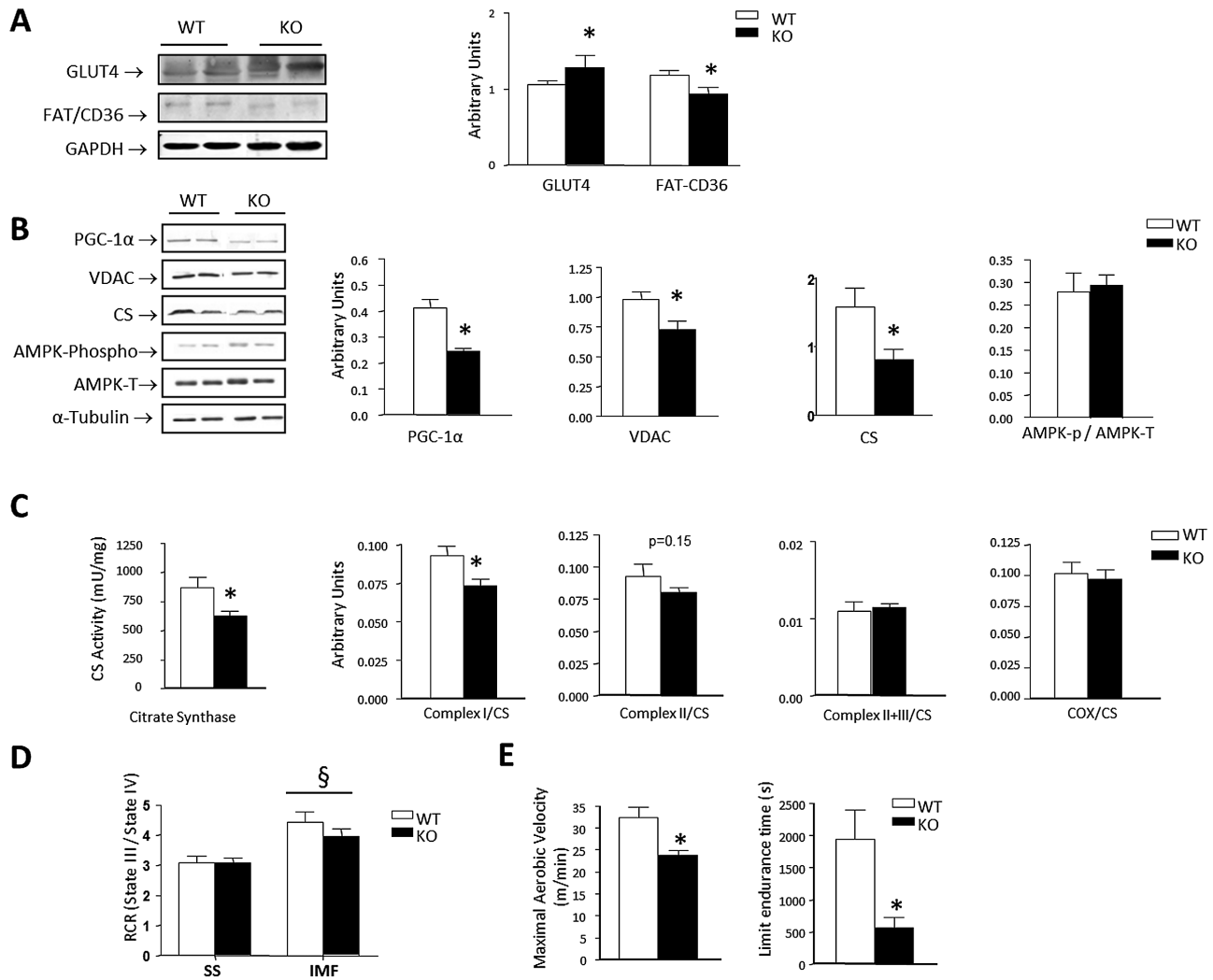


Figure 1. Substrate transporters, mitochondrial function and muscle function in aged *mstn* KO and WT muscle. **(A and B).** Representative immunoblots and quantifications showing protein expression levels of the transporters GLUT4 and FAT-CD36 **(A)** and of PGC1-α, of the outer-membrane mitochondrial protein VDAC, of CS and AMPK phosphorylation **(B)** within the EDL of aged WT and *mstn* KO mice. All protein expression quantifications are normalized to α-Tubulin or GAPDH. **(C).** Enzymatic activity of citrate synthase and mitochondrial complexes were reported in gastrocnemius muscle homogenates. Mitochondrial complexes activities are normalized to CS activity and are expressed in AU. **(D).** Mitochondrial respiration in SS and IMF subfractions of WT and KO muscles was assessed in glycolytic muscle mix (tibialis, anterior gastrocnemius, quadriceps) and RCR was calculated, as the ratio of oxygen consumption at state 3 over oxygen consumption at state 4. Whole body performance is represented by **(E)** maximal running velocity and limit endurance time. Data are expressed as means ± SEM. AU: Arbitrary Units; U/mg: units of activity per mg of total muscular protein; CS: Citrate Synthase; RCR: respiratory control ratio; SS: subsarcolemmal; IMF: intermyofibrillar; * $p < .05$ KO versus WT (t -test genotype effect), § $p < .01$ IMF versus SS (ANOVA type of mitochondria effect); $n = 5-8$.

mitochondrial membrane channel VDAC and of the citrate synthase (CS) **(Figure 1B)**, two markers of mitochondrial content.

To further characterize the mitochondrial phenotype, we performed enzymatic activity measurements on whole muscle and respiratory analyses on isolated mitochondria. Our results showed a

30% lower CS activity in aged *mstn* KO mice compared to aged WT mice **(Figure 1C)**. Furthermore, complex I activity was significantly reduced in aged *mstn* KO mice, whereas no change was observed in the activity of other ETC complexes (complexes II, II+III, COX; **Figure 1C**). For mitochondrial respiration measurements, we choose

to divide mitochondria into their two subpopulations: the subsarcolemmal (SS) and the intermyofibrillar (IMF) mitochondria. As expected, we found higher states 4 and 3 respiration rates for IMF subfraction (data not shown), associated with an increase of RCR, compared to SS in both genotype, ($p < .001$, Figure 1D). We did not observe any differences in mitochondrial respiration parameters (states 4 and 3) as well as in RCR between the two genotypes (not shown and Figure 1D). Similarly, the protein expression of mitochondrial respiratory chain complexes (complexes I, II, III, and V) normalized to VDAC expression were not altered in aged KO compared to WT mice (Supplementary Figure S1).

To assess muscle performance, we subjected aged WT and *mstn* KO mice to physical exercise tests, wherein we measured the maximal aerobic running velocity (MAV) and endurance capacity (time to exhaustion). The aged *mstn* KO mice showed a significant reduction of MAV (~26%) and endurance capacity (~70%) compared to aged WT mice (Figure 1E).

Muscle Autophagic Process is Preserved in Aged KO Mice

We profiled key regulators of autophagy in the EDL muscles from old KO *mstn* and WT samples. Here, we studied protein levels of p62 (receptor for cargo destined to be degraded by autophagy), beclin-1

(a component of the class III phosphoinositide 3-kinase complex involved in the initiation of autophagosomes), LC3-II (the lipidated form of LC3 that is generated during the process of autophagosome formation) and the ratio LC3-II to LC3-I.

We found that all these autophagic markers were unaltered in aged *mstn* KO EDL muscles compared to aged WT (Figure 2).

AICAR Treatment Had No Beneficial Effect on Running Capacity and Muscle Oxidative Metabolism in Aged WT Mice

The MAV and the endurance capacity were not changed with AICAR treatment in aged WT mice (Figure 3). To determine whether AICAR treatment activated AMPK pathway, we first checked AICAR effects on AMPK and ACC phosphorylation as well as on PGC-1 α expression in EDL muscle homogenates of WT mice. AICAR treatment induced a slight but significant increase in PGC-1 α protein levels in WT mice (1.15 fold ie +15% vs placebo; Figure 4A), while it failed to increase others markers of oxidative mitochondrial metabolism. Indeed, AICAR had no effect either on AMPK phosphorylation or on protein level of CS, VDAC (Figure 4A) and representative ETC complex components (Supplementary Figure S1). No AICAR effect was observed on GLUT4 and FAT/CD36 protein expression (Figure 4B). Moreover,

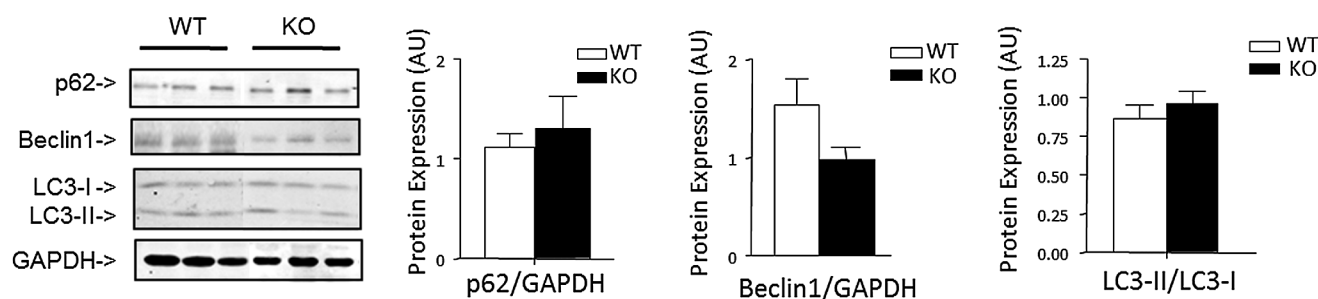


Figure 2. Autophagy markers in EDL from aged WT and KO *mstn* mice. Representative immunoblots and quantifications showing protein expression levels of autophagy markers p62, Beclin1 and LC3 in WT and *mstn* KO mice. All protein expression quantifications are normalized to GAPDH. Data are expressed as means \pm SEM. AU: Arbitrary Units; $n = 5-8$.

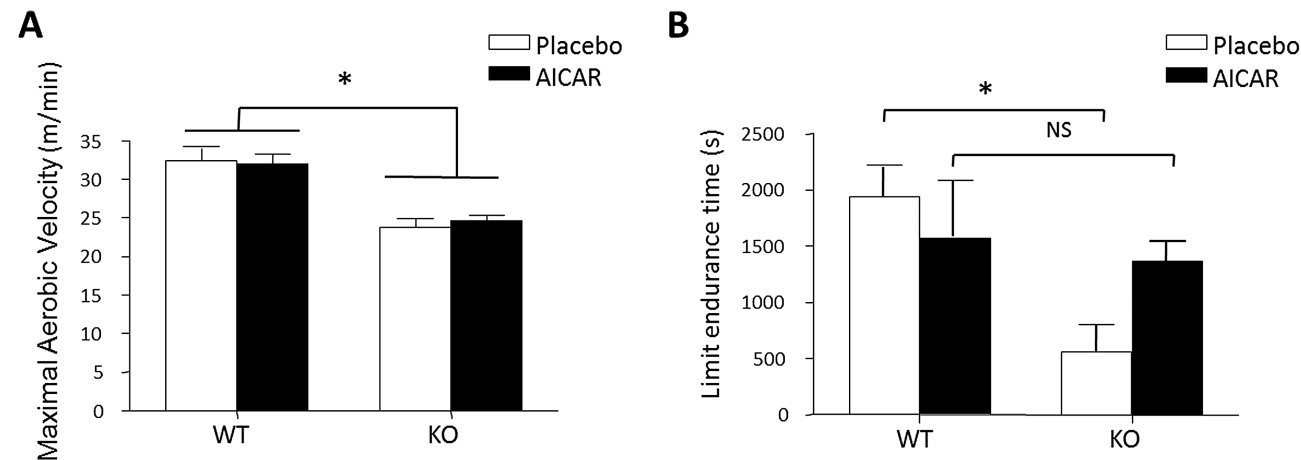


Figure 3. Aerobic running performance in aged *mstn* KO and WT mice without and with AICAR treatment. (A) Maximal running velocity. Data are expressed as means \pm SEM; ANOVA analysis indicated a significant main genotype effect, $* p < .05$ KO versus WT; $n = 11-14$. (B) Limit endurance time. Data are expressed as means \pm SEM; ANOVA analysis indicated a significant main genotype effect and a significant interaction effect between treatment and genotype, $* p < .05$ KO versus WT; $n = 5-8$.

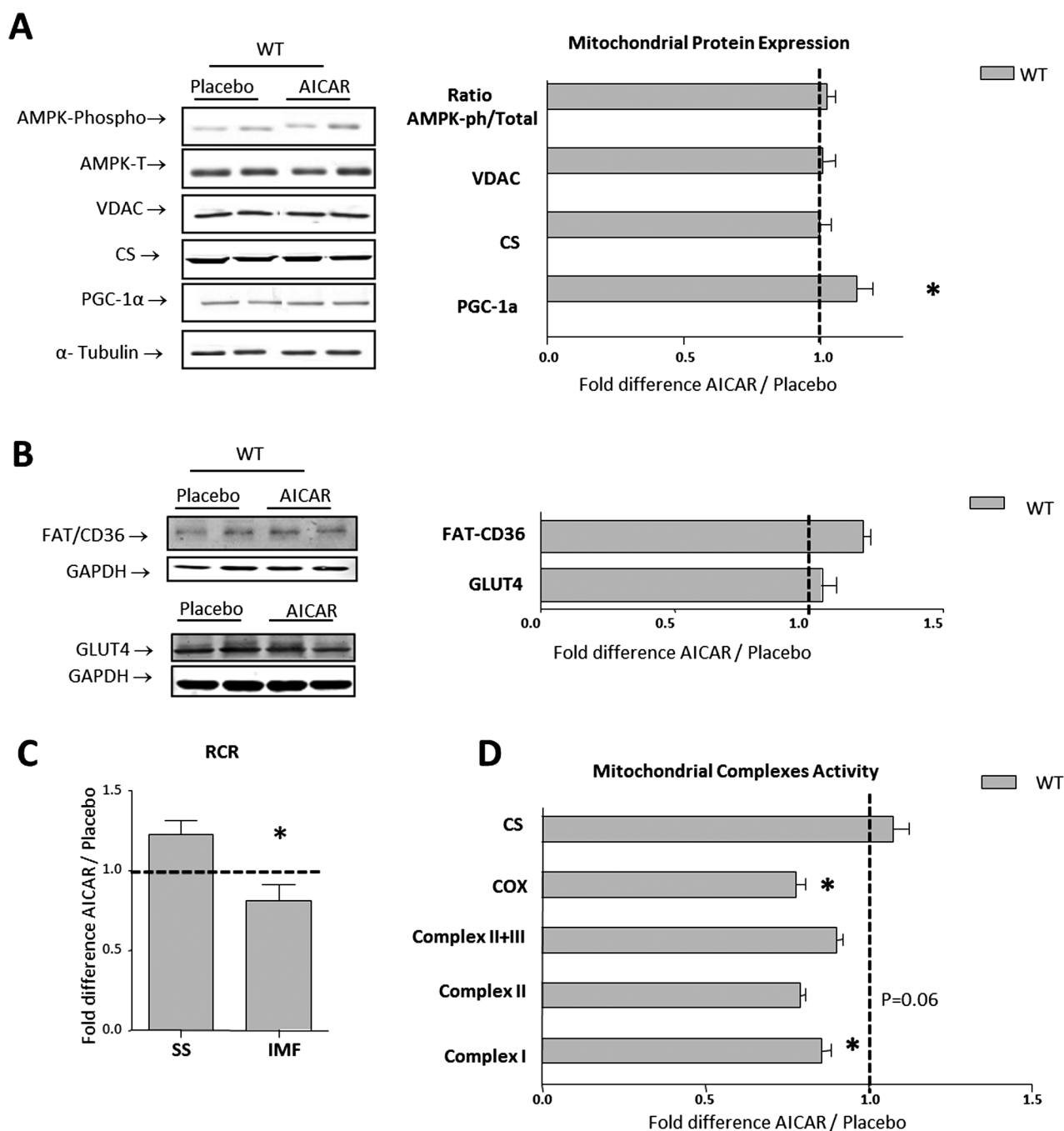


Figure 4. Effect of AICAR treatment on mitochondrial function on aged WT mice. **(A).** Representative Western blots and graphical summary of phosphorylated and total forms of AMPK, VDAC, CS and of PGC1-α within the EDL of aged WT treated (AICAR) or untreated (placebo). **(B).** Representative immunoblots and quantifications showing protein expression levels of the transporters GLUT4 and FAT-CD36 **(C).** Mitochondrial respiration in SS and IMF subfractions of WT and KO glycolytic muscles was assessed and RCR is presented. **(D).** Enzymatic activities of mitochondrial complexes after AICAR treatment was reported in gastrocnemius muscle. Data are normalized to citrate synthase activity. AU: Arbitrary Units; U/mg: units of activity per mg of total muscular protein; COX, cytochrome c oxidase; RCR: respiratory control ratio, as the ratio of oxygen consumption at state 3 over oxygen consumption at state 4; SS: subsarcolemmal; IMF: intermyofibrillar. ANOVA analyzed data which were presented in 2 different figures (WT: [Figures 4 and 5](#); KO: [Figures 6 and 7](#)). ANOVA analysis indicated significant main treatment effect on PGC-1-α protein levels and RCR, and statistical interaction between treatment and genotype for mitochondrial complexes activity. In this figure, data are presented as the fold increase in AICAR over Placebo group in WT mice. The dashed line represents the no-effect control value (1); * $p < .05$ AICAR versus Placebo; $n = 5-8$.

AICAR induced a decrease in complex I and COX enzyme activity and in RCR values in IMF mitochondrial fractions ($p < .05$, [Figure 4C and D](#)). Lastly, autophagy markers were not modified by the treatment ([Figure 5](#)).

AICAR Treatment Improved Aerobic Running Performance in Aged KO *mstn* Mice

AICAR treatment did not change MAV ([Figure 3A](#)), but reduced differences in running endurance parameters between aged KO and WT

mice (Figure 3B). Indeed, aged KO mice endurance time increased from 30% (placebo) to 87% (AICAR) of WT values.

AICAR Treatment Boosted PGC-1 α Protein Expression in Aged *mstn* KO Muscles and Activity of All Mitochondrial Electron Transport Chain Complexes

AICAR treatment induced a greater increase in PGC-1 α protein expression in aged KO mice (+1.50 fold ie +50% vs placebo; Figure 6A) compared to WT mice (+1.15 fold ie + 15 % vs placebo; Figure 4A). However, AICAR did not activate phosphorylation of AMPK (Figure 6A) and ACC (data not shown). The treatment also failed to change the glycolytic phenotype with no significant increase in GLUT4 and FAT/CD36 (Figure 6B) expression in aged muscle tissues of KO mice ($p = .27$ and $.13$ respectively). In addition, AICAR treatment did not affect mitochondrial density since neither CS activity (Figure 6D), nor CS, VDAC (Figure 6A) and mitochondrial respiratory chain complex subunits protein expression (Supplementary Figure S1) were altered. We further examined whether AICAR treatment affected mitochondrial function in aged *mstn* KO mice with measurement of mitochondrial respiration. AICAR decreased RCR in IMF mitochondria of aged *mstn* KO mice ($p < .05$) (Figure 6C). Lastly, activities of all ETC complexes were significantly increased with AICAR in aged *mstn* KO mice compared to aged WT mice (Figure 6D), showing a differential effect of AICAR between the two genotypes. Lastly, Beclin1, LC3II/I and p62 protein contents remained stable suggesting no upregulation of autophagy pathway in aged *mstn* KO mice after 4 weeks of AICAR treatment (Figure 7).

Discussion

Initially, therapies in the skeletal muscle aging focused on the prevention of age-related muscle loss, among them the successful and promising myostatin inhibition pathway. However, recent studies in young mice highlighted that side effect of such therapy is a functional and aerobic metabolic deficit (15–18). How to preserve simultaneous muscle mass and function in ageing muscle? Our study is the first to evaluate in *mstn* hypertrophy mice the ability of AICAR to produce exercise-like effects in ageing skeletal muscle. We showed that *mstn* inhibition and aerobic metabolism activators should be co-developed for delaying age-related deficits in skeletal muscle.

Due to the rapid aging of the population and the inevitable financial pressure on the health care system, a considerable effort is being expanded to develop anti-age and anti-sarcopenic therapies (8,32).

Increasing muscle mass through the control of myostatin-mediated signaling is an attractive strategy since it involves manipulating a naturally occurring mechanism to control muscle mass (8). Our present study confirmed that *mstn* deficiency has a beneficial effect on muscle mass that persists with aging (4,8). Although maintenance of muscle mass is important for muscle function in aged individuals, muscle metabolism is also relevant. Indeed, at the subcellular levels, aged muscle fibers display an increased level of mitochondrial abnormalities and susceptibility to apoptosis (33,34). We provided here for the first time evidence that mitochondrial content/biogenesis remains depreciated in aged *mstn* KO glycolytic muscle with CS activity, VDAC, and PGC-1 α protein content being reduced, as shown previously in young *mstn* KO animals (5,15,35). Recent studies have shown increased AMPK activity in skeletal muscle of young *mstn* KO mice (36,37). Here we reported that this increase is not maintained with aging since neither basal AMPK nor ACC phosphorylation were altered in aged *mstn* KO EDL compared to aged WT mice. Next, we examined the mitochondrial function in aged *mstn* KO and our results suggest that difference tends to diminish somewhat with age. Indeed, complex I activity in gastrocnemius was significantly reduced in aged *mstn* KO mice compared to aged WT. But, with aging, we no longer observed the increased of the COX activity previously shown in young *mstn* KO versus WT mice (15). Furthermore, no difference was found in RCR values of mix glycolytic muscles between genotypes. According to Galuzzi and colleagues (25), mitochondrial content and function are in part controlled by the autophagic process. Indeed, damaged or partially permeabilized mitochondria are selectively degraded by the autophagic machinery, a physiological mechanism that is critical for the maintenance of intracellular homeostasis. In the present study, we did not find a strong case for autophagy being clearly activated at a greater level in aged *mstn* KO EDL muscles, which corroborates results recently published on autophagic gene expression markers in old mice after 7 weeks of post-natal myostatin inhibition (8). Lastly, aerobic endurance performance of aged KO mice remains largely inferior to WT. This exercise intolerance could likely not be related to body weight difference, as Savage and colleagues (14) showed exercise capacity reduction in young *mstn* mice while body weights were similar to those of WT. In the same line, according to Morissette and colleagues (10), a negative effect of *mstn* inactivation on the myocardium could be excluded. The exercise intolerance is thus likely related to the metabolic status of skeletal muscle, ones consistent with the decrease in mitochondrial content/biogenesis markers. This last result is a concern as increased skeletal muscle fatigability promotes the cycle of deconditioning and sedentary lifestyle with

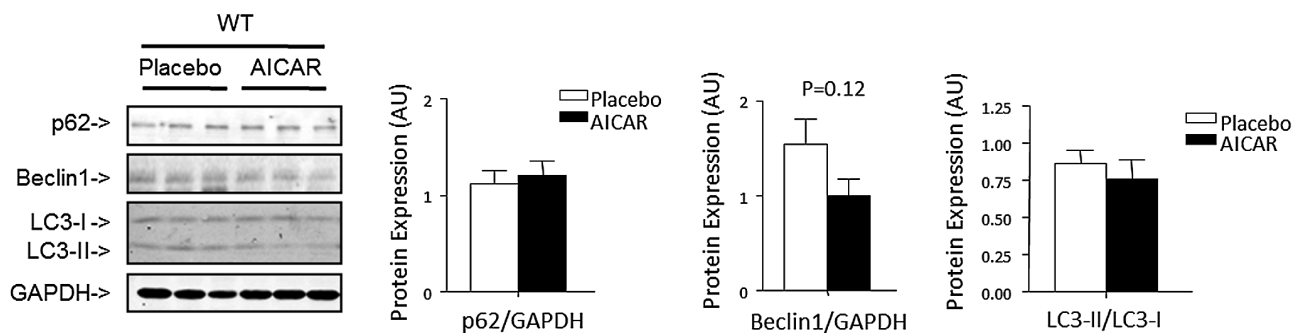


Figure 5. Effect of AICAR treatment in aged WT mice on autophagy. Representative immunoblots and quantifications showing protein expression levels of autophagy markers p62, Beclin1 and LC3II/I) in AICAR or Placebo WT mice. All protein expression quantifications are normalized to GAPDH. Data are expressed as means \pm SEM. No significant ANOVA effect has been observed; $n = 5-8$.

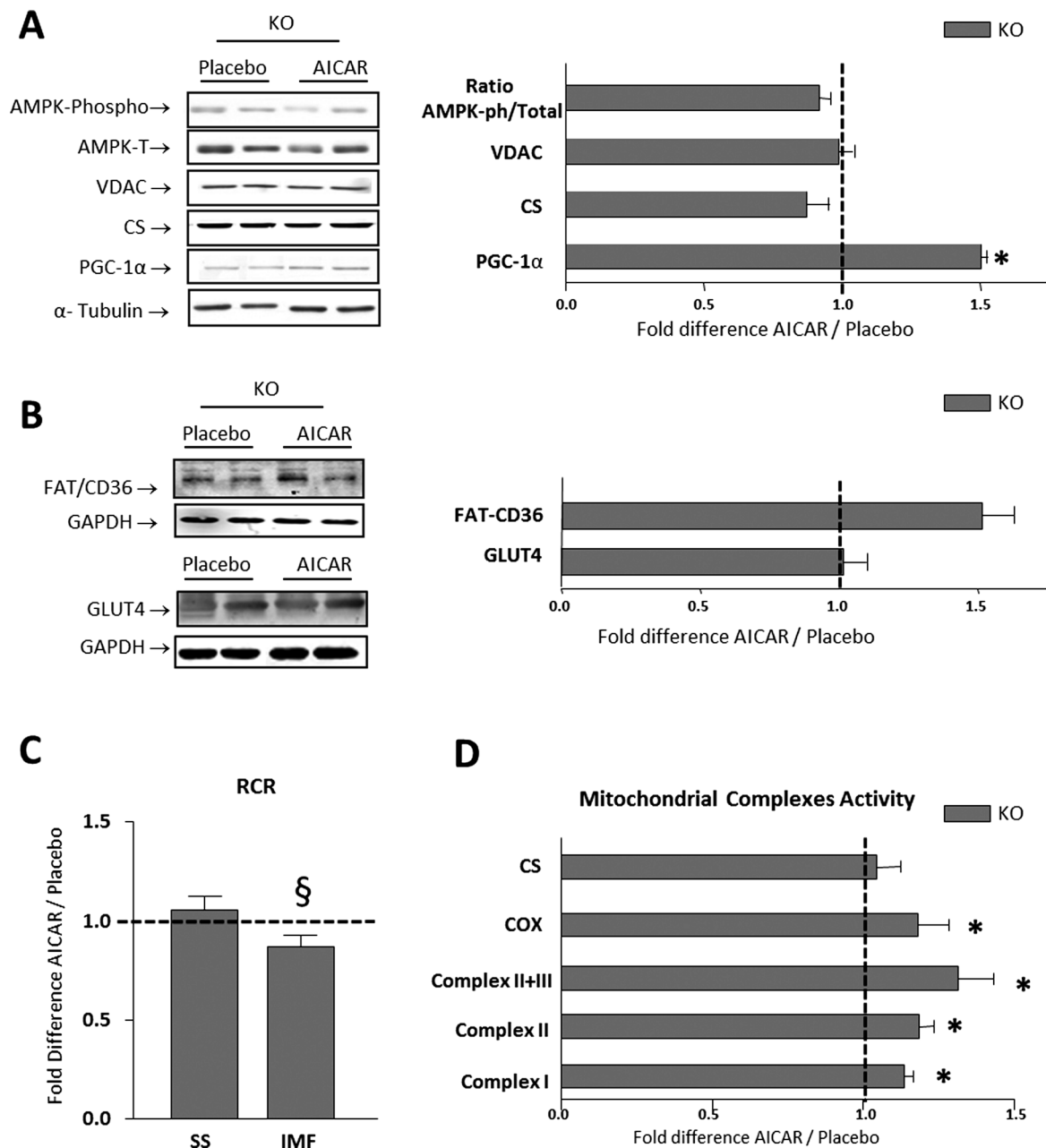


Figure 6. Effect of AICAR treatment on mitochondrial function in aged KO mstn mice. Representative immunoblots and quantifications showing (A) ratio of phosphorylated to total forms of AMPK, VDAC, Citrate Synthase and PGC1- α (B) and protein expression levels of the transporters GLUT4 and FAT-CD36 within the EDL of aged mstn KO mice after AICAR treatment. All protein expression quantifications are normalized to α -Tubulin or GAPDH. (C). Mitochondrial respiration in SS and IMF subfractions of mstn KO glycolytic muscles was assessed and RCR is presented. (D) Enzymatic activities of mitochondrial complexes after AICAR treatment was reported in gastrocnemius muscle homogenate. COX, cytochrome c oxidase; RCR: respiratory control ratio, as the ratio of oxygen consumption at state 3 over oxygen consumption at state 4; SS: subsarcolemmal; IMF: intermyofibrillar. ANOVA analyzed data which were presented in 2 different figures (WT: Figures 4 and 5; KO: Figures 6 and 7. ANOVA analysis indicated significant main treatment effect on PGC-1- α protein levels and RCR, and statistical interaction between treatment and genotype for mitochondrial complexes activity. In this figure, data are presented as the fold increase in AICAR over Placebo group in KO mice. The dashed line represents the no-effect control value (1); § and * $p < .05$ AICAR versus Placebo; $n = 5-8$.

aging, which consequently contributes to a decrease in quality of life, functional independence and higher rates of comorbidities, and mortality (38–40). In humans, mstn inhibition strategy has to take place in mature skeletal muscle. Interestingly, our results highlight those obtained after post-natal mstn inhibition showing a downregulated oxidative phosphorylation and mitochondrial function pathway (16,41). Finally, Collins-Hooper and colleagues (8) showed in

aged mice, that AAV8MyoPPT an antagonizing myostatin signaling by the overexpression of the myostatin propeptide, is associated with a decrease in the number of SDH-positive fibers.

Our results underline the need to target muscle fiber size, by means of myostatin inhibition and oxidative metabolism simultaneously, for further investigation related to age-related muscle weakness (12). Previous positive results in mice suggest that exercise training

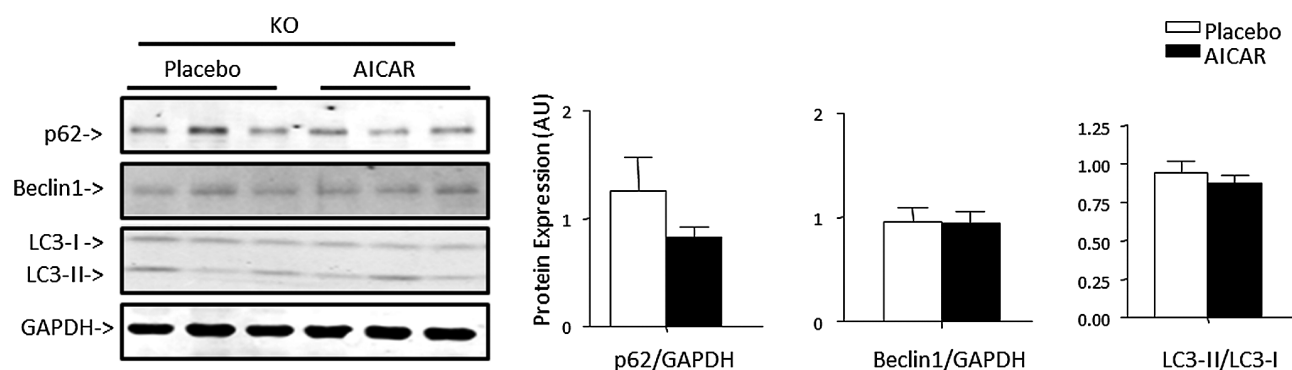


Figure 7. Effect of AICAR treatment in EDL from aged KO mstn mice on autophagy. Representative immunoblots and quantifications showing protein expression levels of autophagy markers p62, Beclin1 and LC3II/I in treated (AICAR) or not treated (placebo) mstn KO mice. All protein expression quantifications are normalized to GAPDH. Data are expressed as means \pm SEM; no significant ANOVA effect has been observed; $n = 5-8$.

could achieve this aim (17,18). In such conditions as age, the use of exercise mimetic drug may represent an interesting alternative therapeutic strategy to boost aerobic metabolism (17). We used AICAR treatment to optimize exercise capacity and oxidative metabolism in aged mice according to Narkar and colleagues (19). As in this previous study, our work demonstrated that AICAR treatment did not alter mitochondria content, but increased PGC-1 α expression in aged WT and KO mice proving the activation of mitochondrial biogenesis signaling. However, contrary to young mice, no AICAR effect on running performance is observed in aged WT mice. Thus, our results do not support that AICAR could be considered as a “mimetic of exercise” in aged WT mice. This result has to be treated with caution since pharmacological phenotypic modifiers and exercise mimetics represent currently a new research dynamic (19,42). AICAR treatment even seems to have several deleterious effects on mitochondrial function in aged WT mice with both decrease of respiratory complexes activity (COX and complexe I) and RCR, indicating a decrease of mitochondrial quality. The decrease of RCR after AICAR treatment is an indicative of lower amounts of ATP per oxygen consumed. Recent findings have also shown that acute AICAR exposure in C2C12 myotubes and adult single skeletal muscle fibers inhibited oxygen consumption (43). This original result is worthy of further mechanistic investigation. Otherwise, our study underscores a beneficial AICAR effect on running endurance capacity in aged mstn KO mice. Indeed, AICAR treatment increased running limit time by 105% in mstn KO mice. AICAR did not alter body and heart weights in our mice suggesting no significant body composition or cardiac effects (44). To investigate the mechanism of the improvement of muscle performance in mstn KO mice, we first explore the mitochondrial function. We can notice that the increase in PGC-1 α is greater in aged mstn KO mice compared to aged WT suggesting greater sensitivity to AICAR treatment. This better responsiveness could be attributed to the muscle type II phenotype of mstn KO mice, since AICAR is known to be more potent in fast-twitch muscles (45). In our present study, we observed a lack of stimulation of basal AMPK phosphorylation one hour after the last AICAR injection. Consistently, several studies reported no increase in AMPK activity after AICAR administration in old rats (46,47). In our work, first the possibility of a missed activation of AMPK pathway due to its transiency could be considered. Second, we cannot also totally exclude the possibility that AICAR could exert its effects on PGC-1 α independently of AMPK activation (48). Whatever the exact mechanisms, in the present study AICAR treatment did not significantly increase mitochondrial pool or substrate transporters. We

can hypothesize that the activation of PGC-1 α expression observed was likely not sufficient to increase it (22).

Data on mitochondrial function are more contradictory. Indeed, the decrease in RCR of IMF mitochondria was accompanied by an increase in the activities of all electron transport chain complexes (activities normalized to CS, to ensure an equal mitochondrial content). These results suggest that, mitochondrial activity can be upregulated by AICAR, to supply the initial deficit of mitochondria density in aged mstn KO mice contrary to WT mice. By increasing the ETC complex activities, mitochondria could produce more energy needed to ensure muscular contraction. On the other hand, AICAR effect on mitochondrial activity may promote autophagy pathway (26). Indeed, the autophagic process is the sole known mechanism for mitochondrial turnover, and clearance of damaged mitochondrial (25). In our present work, we showed no impact of AICAR treatment on autophagy markers suggesting an autophagic independent mechanism. Collectively, we suggest that 4-weeks of AICAR treatment in old mstn KO mice affects positively first mitochondrial ETC complexes activity and prevent from age-related muscle endurance deterioration. The marked increase of PGC-1 protein levels, without an increase in the mitochondria pool, highlights the requirement for a long-term treatment, often over several months. Finally, we cannot rule out the possibility that AICAR acts, directly or indirectly, on other mechanisms such as calcium homeostasis. Indeed, recent findings have shown that AICAR exposure in skeletal muscle of RyR1 mutant mice, independently of the AMPK pathway, reduced Ca²⁺ leak from the sarcoplasmic reticulum to the sarcoplasm (49). New studies and further investigations are needed to demonstrate this hypothesis in mstn KO mice skeletal muscle.

In conclusion, the present study confirms that myostatin inhibition represents an effective anti-atrophic therapeutic strategy in aging. However, it reveals the acute need for simultaneous oxidative metabolism upregulation, as we demonstrate negative metabolic and mitochondrial consequences of mstn inactivation in old mice. We show that 4-weeks AICAR treatment induces some positive effects on muscle glycolytic fast contractile profile of KO mstn mice, with an improvement of endurance running capacity, but not in aged wild-type mice. These results suggest that pharmacological aerobic metabolism activators have to be recognized, not as “miracle molecules” but as “promising molecules” for a new active field of research for aging biology. This study underlines the relevance of aged muscle remodeling by complementary approaches that impact both muscle mass and function, and suggests that mstn inhibition

and aerobic metabolism activators should be co-developed for delaying age-related deficits in skeletal muscle.

Funding

This study was supported by funds from the Institut National de la Recherche Agronomique (INRA) and from the University of Montpellier 1. M.P. is the recipient of doctoral fellowship financed by national Ministry of Higher Education and Research.

Acknowledgments

We thank Sylvain Cerda, Wendy Levrat and Christelle Bertrand-Gaday for the care of the animals used in the present study. The authors are grateful to Ayesha Saleem (McMaster University, Canada) for critical reading and helpful comments on the manuscript.

References

- Schuelke M, Wagner KR, Stolz LE, et al. Myostatin mutation associated with gross muscle hypertrophy in a child. *N Engl J Med*. 2004;350:2682–2688.
- LeBrasseur NK, Schelhorn TM, Bernardo BL, Cosgrove PG, Loria PM, Brown TA. Myostatin inhibition enhances the effects of exercise on performance and metabolic outcomes in aged mice. *J Gerontol A Biol Sci Med Sci*. 2009;64:940–948.
- Murphy KT, Koopman R, Naim T, et al. Antibody-directed myostatin inhibition in 21-mo-old mice reveals novel roles for myostatin signaling in skeletal muscle structure and function. *FASEB J Off Publ Fed Am Soc Exp Biol*. 2010;24:4433–4442.
- Siriatt V, Platt L, Salerno MS, Ling N, Kambadur R, Sharma M. Prolonged absence of myostatin reduces sarcopenia. *J Cell Physiol*. 2006;209:866–873.
- Amthor H, Macharia R, Navarrete R, et al. Lack of myostatin results in excessive muscle growth but impaired force generation. *Proc Natl Acad Sci USA*. 2007;104:1835–1840.
- Mendias CL, Marcin JE, Calderon DR, Faulkner JA. Contractile properties of EDL and soleus muscles of myostatin-deficient mice. *J Appl Physiol* (1985). 2006;101:898–905.
- Schirwis E, Agbulut O, Vadrot N, et al. The beneficial effect of myostatin deficiency on maximal muscle force and power is attenuated with age. *Exp Gerontol*. 2013;48:183–190.
- Collins-Hooper H1, Sartori R, Macharia R, et al. Propeptide-mediated inhibition of myostatin increases muscle mass through inhibiting proteolytic pathways in aged mice. *J Gerontol A Biol Sci Med Sci*. 2014;69:1049–1059.
- Jackson MF, Luong D, Vang DD, et al. The aging myostatin null phenotype: reduced adiposity, cardiac hypertrophy, enhanced cardiac stress response, and sexual dimorphism. *J Endocrinol*. 2012;213:263–275.
- Morissette MR, Stricker JC, Rosenberg MA, et al. Effects of myostatin deletion in aging mice. *Aging Cell*. 2009;8:573–583.
- Correa-de-Araujo R, Hadley E. Skeletal muscle function deficit: a new terminology to embrace the evolving concepts of sarcopenia and age-related muscle dysfunction. *J Gerontol A Biol Sci Med Sci*. 2014;69:591–4.
- Matsakas A. Myostatin tilts the balance between skeletal muscle size, function and metabolism. *Exp Physiol*. 2014;99:469–470.
- Lipina C, Kendall H, McPherron AC, Taylor PM, Hundal HS. Mechanisms involved in the enhancement of mammalian target of rapamycin signalling and hypertrophy in skeletal muscle of myostatin-deficient mice. *FEBS Lett*. 2010;584:2403–2408.
- Savage KJ, McPherron AC. Endurance exercise training in myostatin null mice. *Muscle Nerve*. 2010;42:355–362.
- Ploquin C, Chabi B, Fouret G, et al. Lack of myostatin alters intermyofibrillar mitochondria activity, unbalances redox status, and impairs tolerance to chronic repetitive contractions in muscle. *Am J Physiol Endocrinol Metab*. 2012;302:E1000–1008.
- Relizani K, Mouisel E, Giannesini B, et al. Blockade of ActRIIB signaling triggers muscle fatigability and metabolic myopathy. *Mol Ther*. 2014;22:1423–1433.
- Matsakas A, Mouisel E, Amthor H, Patel K. Myostatin knockout mice increase oxidative muscle phenotype as an adaptive response to exercise. *J Muscle Res Cell Motil*. 2010;31:111–125.
- Matsakas A1, Macharia R, Otto A, et al. Exercise training attenuates the hypermuscular phenotype and restores skeletal muscle function in the myostatin null mouse. *Exp Physiol*. 2012;97:125–40.
- Narkar VA1, Downes M, Yu RT, et al. AMPK and PPARdelta agonists are exercise mimetics. *Cell*. 2008;134:405–15.
- Steinberg GR, Macaulay SL, Febbraio MA, Kemp BE. AMP-activated protein kinase—the fat controller of the energy railroad. *Can J Physiol Pharmacol*. 2006;84:655–665.
- Jørgensen SB, Treebak JT, Viollet B, et al. Role of AMPKalpha2 in basal, training-, and AICAR-induced GLUT4, hexokinase II, and mitochondrial protein expression in mouse muscle. *Am J Physiol Endocrinol Metab*. 2007;292:E331–339.
- Leick L, Fentz J, Biensø RS, et al. PGC-1[alpha] is required for AICAR-induced expression of GLUT4 and mitochondrial proteins in mouse skeletal muscle. *Am J Physiol Endocrinol Metab*. 2010;299:E456–465.
- Olesen J, Kiilerich K, Pilegaard H. PGC-1alpha-mediated adaptations in skeletal muscle. *Pflug Arch Eur J Physiol*. 2010;460:153–162.
- Puigserver P, Adelmant G, Wu Z, et al. Activation of PPARgamma coactivator-1 through transcription factor docking. *Science*. 1999;286:1368–1371.
- Galluzzi L, Kepp O, Trojel-Hansen C, Kroemer G. Mitochondrial control of cellular life, stress, and death. *Circ Res*. 2012;111:1198–1207.
- Pauly M, Daussin F, Burelle Y, et al. AMPK Activation Stimulates Autophagy and Ameliorates Muscular Dystrophy in the mdx Mouse Diaphragm. *Am J Pathol*. 2012;181:583–592.
- Grobet LI, Pirottin D, Farnir F, et al. Modulating skeletal muscle mass by postnatal, muscle-specific inactivation of the myostatin gene. *Genesis*. 2003;35:227–38.
- Cogswell AM, Stevens RJ, Hood DA. Properties of skeletal muscle mitochondria isolated from subsarcolemmal and intermyofibrillar regions. *Am J Physiol*. 1993;264:C383–389.
- Srere PA. Citrate synthase: [EC 4 p.1.3.7 Citrate oxaloacetate-lyase (CoA-acylating)]. *Meth Enzymol*. 1969;13:3–11.
- Janssen AJM, Trijbels FJM, Sengers RCA, et al. Spectrophotometric assay for complex I of the respiratory chain in tissue samples and cultured fibroblasts. *Clin Chem*. 2007;53:729–734.
- Rustin P, Chretien D, Bourgeron T, et al. Biochemical and molecular investigations in respiratory chain deficiencies. *Clin Chim Acta Int J Clin Chem*. 1994;228:35–51.
- Demontis F, Piccirillo R, Goldberg AL, Perrimon N. The influence of skeletal muscle on systemic aging and lifespan. *Aging Cell*. 2013;12:943–949.
- Chabi B, Ljubicic V, Menzies KJ, Huang JH, Saleem A, Hood DA. Mitochondrial function and apoptotic susceptibility in aging skeletal muscle. *Aging Cell*. 2008;7:2–12.
- Shigenaga MK, Hagen TM, Ames BN. Oxidative damage and mitochondrial decay in aging. *Proc Natl Acad Sci USA*. 1994;91:10771–10778.
- Baligand C, Gilson H, Ménard JC, et al. Functional assessment of skeletal muscle in intact mice lacking myostatin by concurrent NMR imaging and spectroscopy. *Gene Ther*. 2010;17:328–337.
- Shan T, Liang X, Bi P, Kuang S. Myostatin knockout drives browning of white adipose tissue through activating the AMPK-PGC1α-Fndc5 pathway in muscle. *FASEB J*. 2013;27:1981–1989.
- Zhang C, McFarlane C, Lokireddy S, et al. Myostatin-deficient mice exhibit reduced insulin resistance through activating the AMP-activated protein kinase signalling pathway. *Diabetologia*. 2011;54:1491–1501.

38. Fielding RA, the LIFE Research Group. The lifestyle interventions and independence for elders study: design and methods. *J Gerontol A Biol Sci Med Sci*. 2011;66:1226–1237.
39. Newman AB, Simonsick EM, Naydeck BL et al. Association of long-distance corridor walk performance with mortality, cardiovascular disease, mobility limitation, and disability. *JAMA*. 2006;295:2018–2026.
40. Peterson MJ, Giuliani C, Morey MC, et al.; Health, Aging and Body Composition Study Research Group. Physical activity as a preventative factor for frailty: the health, aging, and body composition study. *J Gerontol A Biol Sci Med Sci*. 2009;64:61–68.
41. Rahimov F, King OD, Warsing LC, et al. Gene expression profiling of skeletal muscles treated with a soluble activin type IIB receptor. *Physiol Genomics*. 2011;43:398–407.
42. Ljubicic V, Burt M, Jasmin BJ. The therapeutic potential of skeletal muscle plasticity in Duchenne muscular dystrophy: phenotypic modifiers as pharmacologic targets. *FASEB J*. 2014;28:548–568.
43. Spangenburg EE, Jackson KC, Schuh RA. AICAR inhibits oxygen consumption by intact skeletal muscle cells in culture. *J Physiol Biochem*. 2013;69:909–917.
44. Cieslik KA, Taffet GE, Crawford JR, Trial J, Mejia Osuna P, Entman ML. AICAR-dependent AMPK activation improves scar formation in the aged heart in a murine model of reperfused myocardial infarction. *J Mol Cell Cardiol*. 2013;63:26–36.
45. Fillmore N, Jacobs DL, Mills DB, Winder WW, Hancock CR. Chronic AMP-activated protein kinase activation and a high-fat diet have an additive effect on mitochondria in rat skeletal muscle. *J Appl Physiol* (1985). 2010;109:511–520.
46. Bayod S, Del Valle J, Lalanza JF, et al. Long-term physical exercise induces changes in sirtuin 1 pathway and oxidative parameters in adult rat tissues. *Exp Gerontol*. 2012;47:925–935.
47. Reznick RM, Zong H, Li J, et al. Aging-associated reductions in AMP-activated protein kinase activity and mitochondrial biogenesis. *Cell Metab*. 2007;5:151–156.
48. Ventura-Clapier R, Garnier A, Veksler V. Transcriptional control of mitochondrial biogenesis: the central role of PGC-1 α . *Cardiovasc Res*. 2008;79:208–217.
49. Lanner JT, Georgiou DK, Dagnino-Acosta A, et al. AICAR prevents heat-induced sudden death in RyR1 mutant mice independent of AMPK activation. *Nat Med*. 2012;18:244–251.